Topological quantum phase transition in individual Fe atoms on MoS_2/Au(111)

G. G. Blesio [1,*] and A. A. Aligia [2]

[1] *Jožef Stefan Institute, Jamova 39, SI-1000 Ljubljana, Slovenia*

[2] *Instituto de Nanociencia y Nanotecnología CNEA-CONICET, Centro Atómico Bariloche and Instituto Balseiro, 8400 Bariloche, Argentina*

(Received 27 January 2023; revised 30 March 2023; accepted 26 June 2023; published 11 July 2023)

In a recent experiment [Trishin *et al.*, Phys. Rev. Lett. **127**, 236801 (2021)], rich physics was observed for Fe atoms on MoS_2/Au(111), characterized by three different behaviors depending on the spectral density of the substrate ρ_c: one dominated by single-ion anisotropy, one by the Kondo effect, and an intermediate one. Based on symmetry and previous works, we show that the appropriate model to describe the system is the anisotropic two-channel spin-1 Kondo model, which has an underlying topological quantum phase transition (TQPT) between an ordinary Fermi liquid (FL) and a topological one with a nontrivial value of the Luttinger integral. Solving the model with the numerical renormalization group, we show that the different behaviors can be explained in a unified fashion as a function of ρ_c and correspond to both FLs and an intermediate regime close to the TQPT in the topological phase. Further experiments should confirm this transition.

DOI: 10.1103/PhysRevB.108.045113

The understanding of the basic physics of systems composed of magnetic atoms or molecules on metallic surfaces has been a subject of great interest in the past two decades. This is motivated by possible promising technological applications in the field of spintronics [1], for which coherent manipulation of the spin is essential [2], and as a test for paradigmatic theories in condensed matter, such as the Kondo effect [3,4]. In its simplest form, the Kondo effect arises when the free electrons of a metallic host completely screen the magnetic moment of an impurity [3].

Several relevant experiments using a scanning tunneling microscope (STM) have been done to study the low-energy electronic structure of systems in which magnetic units were deposited on noble-metal surfaces. The magnetic units were either transition-metal atoms with incomplete d shells [5–14] or molecules containing transition-metal atoms (or other localized electrons) [15–32]. In most of these works, several variants of the Kondo effect are apparent. The theoretical treatments become involved because of the need to accurately treat the Coulomb repulsion in the incomplete d shells, and in many cases, several localized electrons and conduction bands are relevant at low energies, leading to nontrivial interference effects that modify the line shape in the differential conductance $G(V) = dI/dV$, where I is the current and V the voltage applied to the STM tip [33–42].

One of the simplest models when more that one d orbital is involved is the Anderson model with just two localized orbitals coupled by Hund rules to form a spin 1, hybridized with conduction states of the same symmetry, including anisotropy. In the integer valence limit, the model reduces to the anisotropic two-channel spin-1 Kondo model (A2CS1KM) with hard-axis anisotropy D. Rather surprisingly, it was found a few years ago that these models have a topological quantum phase transition (TQPT) between an ordinary Fermi liquid (FL) when D is below a critical value D_c to a topological FL (TFL) for $D > D_c$ [43,44]. At the TQPT, the Luttinger integral jumps from 0 (trivial) to $\pi/2$ (topological) with increasing D, and therefore, for $D > D_c$, the system cannot be adiabatically connected to a noninteracting system, breaking Landau's hypothesis. For this reason, TFL has previously been called non-Landau FL.

For equivalent channels, $D_c \sim 2.5T_K^0$, where T_K^0 is the Kondo temperature for $D = 0$, which increases with increasing $J' = \rho_c J$, where ρ_c is the density of conduction states and J the exchange coupling. The evolution of the spectral density for localized states $\rho(\omega)$ with D for constant T_K^0 is shown in Fig. 11 of Ref. [44] and in Fig. 1 below for constant D and changing J'. For small D/T_K^0, the spectral density has the usual Kondo peak. Increasing D/T_K^0, near the TQPT, $\rho(\omega)$ displays a very narrow peak mounted on a broader peak (the latter characteristic of the two-channel spin-$\frac{1}{2}$ Kondo model [43]). At the TQPT, the narrow peak changes suddenly to a dip as a consequence of the jump of the Luttinger integral. For large D/T_K^0, the spectral density has two steps at $\omega = \pm D$, characteristic of inelastic transitions [the broadening in Fig. 1 for large ω is an artifact of the numerical renormalization group (NRG)]. Similar behavior has been found in other models [45–47].

This theory has been shown to explain in a consistent way relevant experiments that have been interpreted previously using alternative (and sometimes implausible) explanations. For the system of an isolated iron phthalocyanine molecule deposited on a Au(111) surface [FePc/Au(111)] a narrow dip in $G(V)$ near $V = 0$ was observed [19], mounted on a broader peak, which broadens as the Kondo interaction is weakened [25] and is transformed into a narrow peak with an applied magnetic field [29]. These three experiments were explained using the A2CS1KM with two inequivalent channels [48]. A detailed justification of this model for FePc/Au(111) is given

*german.blesio@ijs.si

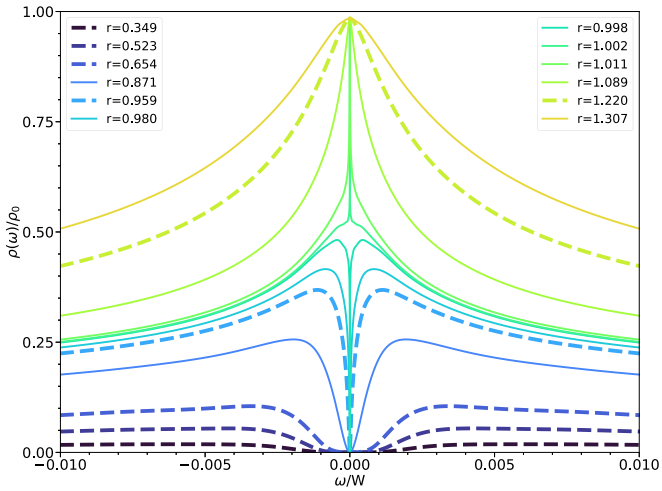

FIG. 1. Spectral density of localized electrons of the anisotropic two-channel spin-1 Kondo model (A2CS1KM) as a function of frequency for several values of $r = J'/J'_c$, where J'_c is the value of J' at the topological quantum phase transition (TQPT), and ρ_0 is the value of $\rho(0)$ predicted by the ordinary Friedel sum rule with vanishing Luttinger integral [48]. Thicker dashed lines correspond to the values of r chosen for the different curves in Fig. 2.

in Ref. [49]. MnPc/Au(111) also shows the transformation of the narrow dip to a narrow peak as a function of an applied magnetic field [30]. The authors proposed an interpretation in terms of a quantum phase transition involving localized singlet states [30]. However, this requires that the singlet be below the triplet by a few millielectronvolts, while in fact the triplet is energetically favored by a Hund's coupling of the order of 1 eV [19].

In the system of nickelocene on Cu(100) [Nc/Cu(100)], as the STM tip approaches the molecule, increasing hybridization between localized and conduction electrons (effectively increasing T_K^0), a transition from a dip in $G(V)$ to a peak is observed [26,50] which was discontinuous in $\frac{2}{3}$ of the cases. The authors have tentatively ascribed the change of behavior to a crossover in the spin of the molecule from 1 in the tunneling regime to $\frac{1}{2}$ in the contact regime. However, the neglected dynamical correlations should lead to a singlet ground state in both cases, and the change in the molecular charge is insufficient to account for the large change in the magnetization. Very recently, the different behaviors were explained in terms of the TQPT [51]. Similar experiments were carried out for iron porphyrin molecules on Au(111) [31,32]. In Ref. [31], the dip narrows in the contact regime instead of turning to a peak, pointing to a weaker hybridization of the localized states with the substrate in comparison with Nc/Cu(100) [31]. However, the transformation from a dip to a peak is observed using a Br-decorated Au(111) surface [32].

A variant of the interaction between magnetic units and metallic surfaces has been realized, introducing thin decoupling layers between both, weakening the hybridization between localized and conduction states [52–56]. Trishin *et al.* [56] considered a system consisting of an Fe atom on top of a monolayer of MoS_2 deposited in turn on a Au(111) surface. Particularly interesting in this system is the fact that MoS_2 on Au(111) forms a Moiré structure, which implies strong local variations of the density of conduction electrons. Therefore, depending on the specific position at which the Fe adatom is located, dramatic variations of the effective exchange between electron localized at the Fe adatom and conduction electrons in the rest of the system take place. The differential conductances $G(V)$ were recorded on nearly 40 different Fe atoms, and six of them are presented in Ref. [56]. We denote the corresponding spectra by the letters (a)–(f) used in Fig. 2 of Ref. [56]. Five of them [(b)–(f)] are reproduced here in Fig. 2. The spectra (a)–(d) contain a dip of variable width in $G(V)$ near $V = 0$. Spectrum (e) contains a narrow dip mounted on a broader peak, and spectrum (f) consists of a single Kondo peak.

Considering that the rigorous study of the A2CS1KM is both recent and difficult, it is understandable that the theoretical part of Ref. [56] was based on more traditional one-channel approaches to explain the different regimes [perturbation theory for (b)–(d) [57], Lorentz peak plus Frota dip (without justification) for (e), and Frota peak for (f)]. However, not only two channels are expected (see below), but also, in a recent experimental study of the same group for Mn atoms, the authors concluded that more than one channel is coupled to the atom [58]. Since Mn is next to Fe on the periodic table, one expects the same to be valid for Fe atoms.

In this paper, we show that all spectra can be semiquantitatively explained using the A2CS1KM with degenerate channels, fixed D and varying $J' = \rho_c J$ assumed the same for both channels. The minor discrepancies are likely due to the dependence on the energy of the conduction density of states ρ_c which we neglect. Since alternative perturbative or diagrammatic approximations fail to describe the TQPT [44], we use the NRG.

The model for the system can be justified on general physical grounds. Density functional theory (DFT) calculations of Fe atoms on freestanding MoS_2 indicate that the spin state of the atoms is either $S = 1$ [59] or $S = 2$ [60]. However, for $S = 2$, one would expect a second jump in $G(V)$ at larger $|V|$ in the regime of low J, which is not observed experimentally [Fig. 3(h) of Ref. [56]]. In addition, in experiment as well as DFT calculations, Fe atoms are located in positions with symmetry corresponding to the point group C_{3v}. Therefore, the Fe $3d$ orbitals are split into one A_1 singlet and two E doublets [61]. Choosing the coordinates in such a way that z is perpendicular to the surface, the $3d$ orbital with symmetry $3z^2$-r^2 transforms as A_1, one E doublet has the form [61]:

$$|x\rangle = \alpha|xz\rangle + \beta|(x^2 - y^2)/2\rangle,$$
$$|y\rangle = \alpha|yz\rangle - \beta|xy\rangle, \quad (1)$$

and the other E doublet has the same form interchanging α with $-\beta$ (so that all states are orthogonal).

It is likely that the spin 1 is formed occupying the two states of an E doublet. Then it is expected that the spin-orbit coupling (SOC) originates hard-axis anisotropy $D(S_z)^2$ with $D > 0$ [51] and that each of the degenerate orbitals of the doublet hybridizes with conduction states of the same symmetry [43,44,51]. In the integer valence limit, this reasoning leads naturally to the A2CS1KM with the same exchange interaction for both channels. In the other case in which one of the orbitals of the spin 1 corresponds to the A_1 symmetry, the SOC favors a particular linear combination of the E states

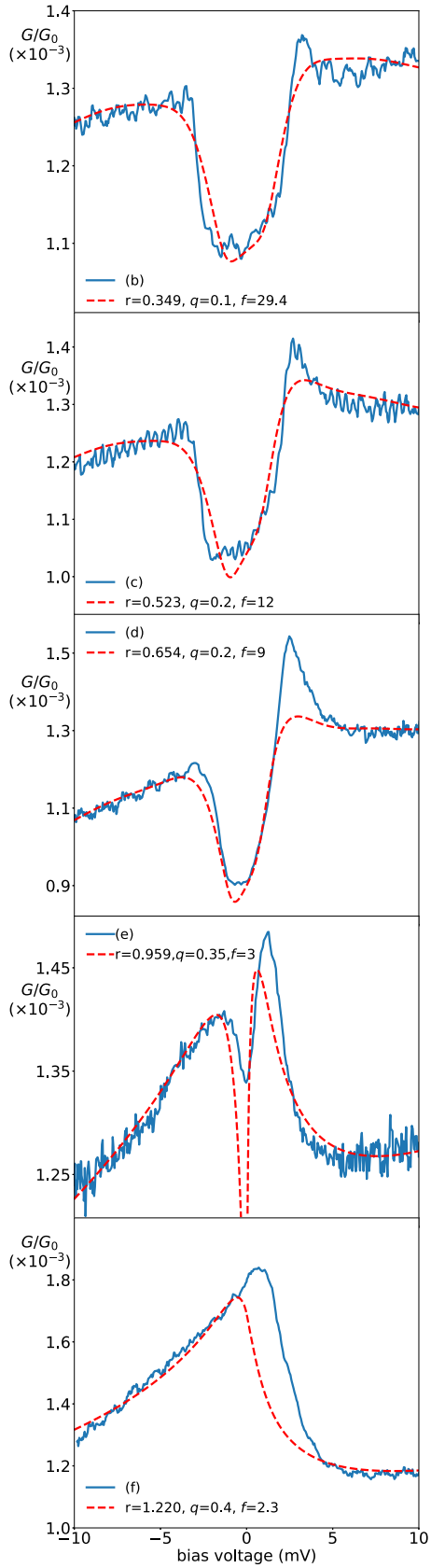

FIG. 2. Differential conductance corresponding to the experimental curves (b)–(f) in Ref. [56] (blue full lines) and the results for our model (red dashed lines). Note that (a) is not included, and the top figure corresponds to (b).

for the other orbital [49], and the low-energy model is also the A2CS1KM but with different exchange interactions for both symmetries. This case corresponds to iron phthalocyanine on Au(111) [48,49]. For the system studied here, we find that very different exchange constants cannot explain the experiments, and then we assume that they are equal. Therefore, the model takes the form:

$$H_K = \sum_{k\tau\sigma} \varepsilon_{k\tau} c^\dagger_{k\tau\sigma} c_{k\tau\sigma} + \sum_{k\tau\sigma\sigma'} \frac{J}{2} c^\dagger_{k\tau\sigma} (\vec{\sigma})_{\sigma\sigma'} c_{k\tau'\sigma'} \cdot \vec{S} + D S_z^2, \tag{2}$$

where $c^\dagger_{k\tau\sigma}$ creates a conduction electron with point-group symmetry τ, spin σ, and remaining quantum numbers k. The first term describes the substrate bands, the second the Kondo exchange with the localized spin $\vec{S}$ with exchange couplings J, and the last term is the single-ion uniaxial magnetic anisotropy.

The numerical calculations were performed with the Ljubljana code of the NRG [62,63]. We assume flat conduction bands extending from $-W$ to W for both symmetries. The density of these states is therefore $\rho_c = 1/(2W)$. We take $W = 1$ eV, $D = 2.7$ meV, and assume that J varies depending on the Fe position. In the real system, ρ_c depends on the position of the Fe adatom, but the relevant parameter is the adimensional product $J' = \rho_c J$. The TQPT is at $J'_c \sim 0.135$. For the sake of clarity, the different curves are shown for different values of the ratio $r = J'/J'_c$, which is the main variable in what follows.

We assume that the structure at low voltage V in the differential conductance $G(V) = dI/dV$ is determined by the localized and conduction electrons of symmetry τ included in the model and that the STM tip senses mainly the localized $3d$ states with some admixture of conduction states. Then the contribution of the model to $G(V)$ at zero temperature is (except for a factor f included below) [48]

$$G_m(V) = -\big[(1-q^2)\mathrm{Im}G^d_{\tau\sigma}(\omega) + 2q\mathrm{Re}G^d_{\tau\sigma}(\omega)\big], \tag{3}$$

where $G^d_{\tau\sigma}(\omega)$ is the Green's function of localized electrons for symmetry τ and spin σ (which depends only on J'), and q is a measure of the contribution of the conduction states. In the experimental spectrum, there is also a linear background due to the contribution of other states, and $G_m(V)$ is affected by a factor f which depends on the distance of the STM tip from the system. Thus, we take

$$G(V) = f G_m(V) + A + B\omega. \tag{4}$$

This expression contains only five parameters, but the shape of each curve depends mainly on r and to a lesser extent on q. The fact that both r and q increase in going from (b) to (f) is consistent with the reported greater density of conduction states.

In Fig. 2, we represent the experimental curves (b)–(f) obtained from Fig. 2 of Ref. [56] and the corresponding result from our theory. We have not included the curve (a), which is similar to a rectangular dip formed by two steplike functions, because these steps are overbroadened in our calculations due to technical reasons that limit the resolution of the NRG at large energies [64]. We have not attempted to fit the data, but rather we have chosen parameters (particularly r) that provide semiquantitative agreement. The assumption of a constant density of conduction states and the effect of other orbitals not contained in our model should affect a realistic comparison

with experiment. Our aim is to show that the same model can explain the different behaviors observed.

Experimentally, the figures can be divided into those belonging to a regime dominated by the anisotropy D in which Kondo interactions can be treated perturbatively [curves (a)–(c)], curve (f) where Kondo exchange J dominates which can be fitted by a simple Frota line shape, and an intermediate regime [curves (d) and (e)]. For curve (f), a Frota fitting is better than our result, mainly because the former has the freedom of locating the position of the peak, which our theory does not have. This can be improved allowing intermediate valence. It is known that a smaller occupancy of the localized states shifts the Kondo peak to higher energies. A higher J' implies a higher hybridization between localized and conduction states, and this implies a higher degree of intermediate valence. However, we want to keep the model simple, and our goal is to explain all regimes within the same footing rather than to improve minor details for each curve. The dips obtained by our theory for the curves (d) and (e) are deeper than the ones experimentally observed. This might also be an effect of intermediate valence which increases the minimum possible value of the localized spectral density [51].

The intermediate regime, particularly curve (e) with a narrow dip mounted on a broader dip, results naturally from the A2CS1KM (see Fig. 1 for r slightly smaller than 1) but is very hard to explain with alternative theories. Before the study of the A2CS1KM, Minamitani *et al.* [19] found similar behavior in $G(V)$ in FePc/Au(111), which was interpreted as a two-stage Kondo effect: The broad peak would be originated by the Kondo effect for one channel ($3z^2$-r^2 symmetry) and the narrow dip as the second-stage Kondo effect for states of a different symmetry (denoted by π) [65]. A peak indicates dominance of localized states in the tunneling to the STM tip [low q in Eq. (4)] for $3z^2$-r^2 symmetry and dominance of the tunneling to conduction states [large q in Eq. (4)] for π orbitals. However, with this explanation, one would expect a narrowing of both features as the molecule is raised from the surface, contrary to more recent experiments [25], which together with the dependence on the magnetic field [29] could be explained using the A2CS1KM [48]. For Fe atoms on MoS_2/Au(111), the presence of a decoupling layer weakens the tunneling of conduction electrons to the STM tip, and therefore, one expects low q (as used in this paper) and that $G(V)$ reflects mostly the density of Fe states.

To further support the relevance of the A2CS1KM to the system, it would be interesting to perform experiments for ρ_c slightly larger than the corresponding value for curve (e) and still smaller than the corresponding one for curve (f). In this interval, there might be a spectrum with a narrow peak mounted on a broader peak corresponding to r slightly larger than 1. In any case, for curve (e), an applied magnetic field parallel to the anisotropy direction should turn the dip into a peak in a continuous way [48]. This is another smoking gun for the A2CS1KM or its extension to intermediate valence since alternative meaningful explanations do not exist.

In summary, we provide strong arguments that indicate that the appropriate model to describe individual Fe atoms on MoS_2/Au(111) is the A2CS1KM, possibly with some degree of intermediate valence in the regime in which the Kondo exchange dominates. The different observed curves of differential conductances can be explained by the theory modifying the spectral density of the substrate. The model has a TQPT for anisotropy $D_c \sim 2.5T_K^0$, where T_K^0 is the Kondo temperature for $D = 0$. We expect that this paper will stimulate further experiments for conditions near the transition. A fine-tuning of the Fe positions or changes in the substrate, might render it possible to observe a sudden change from a narrow dip to a narrow peak mounted on a broader peak, signaling the TQPT. This sudden change has not yet been observed in similar materials. In any case, applying a magnetic field in the topological phase near the TQPT [curve (e)] should change the narrow dip into a narrow peak, confirming the validity of the model.

We thank Felix von Oppen and Katharina Franke for useful discussions. A.A.A. is supported by PICT 2017-2726 and PICT 2018-01546 of the ANPCyT, Argentina. GGB is supported by the Slovenian Research Agency under Grants No. P1-0044 and No. J1-2458. Part of computation was performed on the supercomputer Vega at the Institute of Information Science in Maribor, Slovenia.

[1] S. A. Wolf, D. D. Awschalom, R. A. Buhrman, J. M. Daughton, S. von Molnár, M. L. Roukes, A. Y. Chtchelkanova, and D. M. Treger, Spintronics: A spin-based electronics vision for the future, Science **294**, 1488 (2001).

[2] K. Yang, W. Paul, S.-H. Phark, P. Willke, Y. Bae, T. Choi, T. Esat, A. Ardavan, A. J. Heinrich, and C. P. Lutz, Coherent spin manipulation of individual atoms on a surface, Science **366**, 509 (2019).

[3] A. C. Hewson, *The Kondo Problem to Heavy Fermions* (Cambridge University Press, Cambridge, 1997).

[4] J. Kondo, Resistance minimum in dilute magnetic alloys, Prog. Theor. Phys. **32**, 37 (1964).

[5] V. Madhavan, W. Chen, T. Jamneala, M. F. Crommie, and N. S. Wingreen, Tunneling into a single magnetic atom: Spectroscopic evidence of the Kondo resonance, Science **280**, 567 (1998).

[6] H. C. Manoharan, C. P. Lutz, and D. M. Eigler, Quantum mirages formed by coherent projection of electronic structure, Nature (London) **403**, 512 (2000).

[7] K. Nagaoka, T. Jamneala, M. Grobis, and M. F. Crommie, Temperature Dependence of a Single Kondo Impurity, Phys. Rev. Lett. **88**, 077205 (2002).

[8] N. Knorr, M. A. Schneider, L. Diekhöner, P. Wahl, and K. Kern, Kondo Effect of Single Co Adatoms on Cu Surfaces, Phys. Rev. Lett. **88**, 096804 (2002).

[9] P. Wahl, L. Diekhöner, M. A. Schneider, L. Vitali, G. Wittich, and K. Kern, Kondo Temperature of Magnetic Impurities at Surfaces, Phys. Rev. Lett. **93**, 176603 (2004).

[10] L. Limot, E. Pehlke, J. Kröger, and R. Berndt, Surface-State Localization at Adatoms, Phys. Rev. Lett. **94**, 036805 (2005).

[11] N. Néel, J. Kröger, L. Limot, K. Palotas, W. A. Hofer, and R. Berndt, Conductance and Kondo Effect in a

Controlled Single-Atom Contact, Phys. Rev. Lett. **98**, 016801 (2007).

[12] L. Vitali, R. Ohmann, S. Stepanow, P. Gambardella, K. Tao, R. Huang, V. S. Stepanyuk, P. Bruno, and K. Kern, Kondo Effect in Single Atom Contacts: The Importance of the Atomic Geometry, Phys. Rev. Lett. **101**, 216802 (2008).

[13] D.-J. Choi, M. V. Rastei, P. Simon, and L. Limot, Conductance-Driven Change of the Kondo Effect in a Single Cobalt Atom, Phys. Rev. Lett. **108**, 266803 (2012).

[14] D.-J. Choi, S. Guissart, M. Ormaza, N. Bachellier, O. Bengone, P. Simon, and L. Limot, Kondo resonance of a Co atom exchange coupled to a ferromagnetic tip, Nano Lett. **16**, 6298 (2016).

[15] P. Wahl, L. Diekhöner, G. Wittich, L. Vitali, M. A. Schneider, and K. Kern, Kondo Effect of Molecular Complexes at Surfaces: Ligand Control of the Local Spin Coupling, Phys. Rev. Lett. **95**, 166601 (2005).

[16] L. Gao, W. Ji, Y. B. Hu, Z. H. Cheng, Z. T. Deng, Q. Liu, N. Jiang, X. Lin, W. Guo, S. X. Du *et al.*, Site-Specific Kondo Effect at Ambient Temperatures in Iron-Based Molecules, Phys. Rev. Lett. **99**, 106402 (2007).

[17] N. Roch, S. Florens, V. Bouchiat, W. Wernsdorfer, and F. Balestro, Quantum phase transition in a single-molecule quantum dot, Nature (London) **453**, 633 (2008).

[18] J. J. Parks, A. R. Champagne, T. A. Costi, W. W. Shum, A. N. Pasupathy, E. Neuscamman, S. Flores-Torres, P. S. Cornaglia, A. A. Aligia, C. A. Balseiro *et al.*, Mechanical control of spin states in spin-1 molecules and the underscreened Kondo effect, Science **328**, 1370 (2010).

[19] E. Minamitani, N. Tsukahara, D. Matsunaka, Y. Kim, N. Takagi, and M. Kawai, Symmetry-Driven Novel Kondo Effect in a Molecule, Phys. Rev. Lett. **109**, 086602 (2012).

[20] Y. Zhang, S. Kahle, T. Herden, Ch. Stroh, M. Mayor, U. Schlickum, M. Ternes, P. Wahl, and K. Kern, Temperature and magnetic field dependence of a Kondo system in the weak coupling regime, Nat. Commun. **4**, 2110 (2013).

[21] J. Kügel, M. Karolak, J. Senkpiel, P.-J. Hsu, G. Sangiovanni, and M. Bode, Relevance of hybridization and filling of 3*d* orbitals for the Kondo effect in transition metal phthalocyanines, Nano Lett. **14**, 3895 (2014).

[22] S. Karan, D. Jacob, M. Karolak, C. Hamann, Y. Wang, A. Weismann, A. I. Lichtenstein, and R. Berndt, Shifting the Voltage Drop in Electron Transport Through a Single Molecule, Phys. Rev. Lett. **115**, 016802 (2015).

[23] T. Esat, B. Lechtenberg, T. Deilmann, C. Wagner, P. Krüger, R. Temirov, M. Rohlfing, F. B. Anders, and F. S. Tautz, A chemically driven quantum phase transition in a two-molecule Kondo system, Nat. Phys. **12**, 867 (2016).

[24] V. Iancu, K. Schouteden, Z. Li, and C. Van Haesendonck, Electron-phonon coupling in engineered magnetic molecules, Chem. Commun. **52**, 11359 (2016).

[25] R. Hiraoka, E. Minamitani, R. Arafune, N. Tsukahara, S. Watanabe, M. Kawai, and N. Takagi, Single-molecule quantum dot as a Kondo simulator, Nat. Commun. **8**, 16012 (2017).

[26] M. Ormaza, P. Abufager, B. Verlhac, N. Bachellier, M.-L. Bocquet, N. Lorente, and L. Limot, Controlled spin switching in a metallocene molecular junction, Nat. Commun. **8**, 1974 (2017).

[27] M. Ormaza, N. Bachellier, M. N. Faraggi, B. Verlhac, P. Abufager, P. Ohresser, L. Joly, M. Romeo, F. Scheurer, M.-L. Bocquet *et al.*, Efficient spin-flip excitation of a nickelocene molecule, Nano Lett. **17**, 1877 (2017).

[28] B. Verlhac, N. Bachellier, L. Garnier, M. Ormaza, P. Abufager, R. Robles, M.-L. Bocquet, M. Ternes, N. Lorente, and L. Limot, Atomic-scale spin sensing with a single molecule at the apex of a scanning tunneling microscope, Science **366**, 623 (2019).

[29] K. Yang, H. Chen, Th. Pope, Y. Hu, L. Liu, D. Wang, L. Tao, W. Xiao, X. Fei, Y.-Y. Zhang *et al.*, Tunable giant magnetoresistance in a single-molecule junction, Nat. Commun. **10**, 3599 (2019).

[30] X. Guo, Q. Zhu, L. Zhou, W. Yu, W. Lu, and W. Lian, Gate tuning and universality of two-stage Kondo effect in single molecule transistors, Nat. Commun. **12**, 1566 (2021).

[31] X. Meng, J. Möller, M. Mansouri, D. Sánchez-Portal, A. Garcia-Lekue, A. Weismann, C. Li, R. Herges, and R. Berndt, Controlling the Spin States of FeTBrPP on Au(111), ACS Nano **17**, 1268 (2023).

[32] Y. Gao, S. Vlaic, T. Gorni, L. de'Medici, S. Clair, D. Roditchev, and S. Pons, Manipulation of the magnetic state of a porphyrin-based molecule on gold: From Kondo to quantum nanomagnet via the charge fluctuation regime, ACS Nano **17**, 9082 (2023).

[33] O. Újsághy, J. Kroha, L. Szunyogh, and A. Zawadowski, Theory of the Fano Resonance in the STM Tunneling Density of States due to a Single Kondo Impurity, Phys. Rev. Lett. **85**, 2557 (2000).

[34] J. Merino and O. Gunnarsson, Role of Surface States in Scanning Tunneling Spectroscopy of (111) Metal Surfaces with Kondo Adsorbates, Phys. Rev. Lett. **93**, 156601 (2004).

[35] A. Aligia, and A. Lobos, Mirages and many-body effects in quantum corrals, J. Phys.: Condens. Matter **17**, S1095 (2005).

[36] C.-Y. Lin, A. H. Castro Neto, and B. A. Jones, First-Principles Calculation of the Single Impurity Surface Kondo Resonance, Phys. Rev. Lett. **97**, 156102 (2006).

[37] A. A. Aligia, Effective Kondo Model for a Trimer on a Metallic Surface, Phys. Rev. Lett. **96**, 096804 (2006).

[38] S. Florens, A, Freyn, N. Roch, W. Wernsdorfer, F. Balestro, P. Roura-Bas, and A. A. Aligia, Universal transport signatures in two-electron molecular quantum dots: Gate-tunable Hund's rule, underscreened Kondo effect and quantum phase transitions, J. Phys.: Condens. Matter **23**, 243202 (2011).

[39] S. Frank and D. Jacob, Orbital signatures of Fano-Kondo line shapes in STM adatom spectroscopy, Phys. Rev. B **92**, 235127 (2015).

[40] D. K. Morr, Theory of scanning tunneling spectroscopy: From Kondo impurities to heavy fermion materials, Rep. Prog. Phys. **80**, 014502 (2017).

[41] P. Roura-Bas, F. Güller, L. Tosi, and A. A. Aligia, Destructive quantum interference in transport through molecules with electron-electron and electron-vibration interactions, J. Phys.: Condens. Matter **31**, 465602 (2019).

[42] J. Fernández, P. Roura-Bas, and A. A. Aligia, Theory of Differential Conductance of Co on Cu(111) Including Co *s* and *d* Orbitals, and Surface and Bulk Cu States, Phys. Rev. Lett. **126**, 046801 (2021).

[43] G. G. Blesio, L. O. Manuel, P. Roura-Bas, and A. A. Aligia, Topological quantum phase transition between Fermi liquid phases in an Anderson impurity model, Phys. Rev. B **98**, 195435 (2018).

[44] G. G. Blesio, L. O. Manuel, P. Roura-Bas, and A. A. Aligia, Fully compensated Kondo effect for a two-channel

spin $S = 1$ impurity, Phys. Rev. B **100**, 075434 (2019).

[45] L. De Leo and M. Fabrizio, Spectral properties of a two-orbital Anderson impurity model across a non-Fermi-liquid fixed point, Phys. Rev. B **69**, 245114 (2004),

[46] O. J. Curtin, Y. Nishikawa, A. C. Hewson, and D. J. G. Crow, Fermi liquids and the Luttinger theorem, J. Phys. Commun. **2**, 031001 (2018).

[47] Y. Nishikawa, O. J. Curtin, A. C. Hewson, and D. J. G. Crow, Magnetic field induced quantum criticality and the Luttinger sum rule, Phys. Rev. B **98**, 104419 (2018).

[48] R. Žitko, G. G. Blesio, L. O. Manuel, and A. A. Aligia, Iron phthalocyanine on Au(111) is a "non-Landau" Fermi liquid, Nat. Commun. **12**, 6027 (2021).

[49] A. A. Aligia, Low-energy physics for an iron phthalocyanine molecule on Au(111), Phys. Rev. B **105**, 205114 (2022).

[50] M. Mohr, M. Gruber, A. Weismann, D. Jacob, P. Abufager, N. Lorente, and R. Berndt, Spin dependent transmission of nickelocene-Cu contacts probed with shot noise, Phys. Rev. B **101**, 075414 (2020).

[51] G. G. Blesio, R. Žitko, L. O. Manuel, and A. A. Aligia, Topological quantum phase transition of nickelocene on Cu(100), SciPost Phys. **14**, 042 (2023).

[52] A. J. Heinrich, J. A. Gupta, C. P. Lutz, and D. M. Eigler, Single-atom spin-flip spectroscopy, Science **306**, 466 (2004).

[53] C. F. Hirjibehedin, C.-Y. Lin, A. F. Otte, M. Ternes, C. P. Lutz, B. A. Jones, and A. J. Heinrich, Large magnetic anisotropy of a single atomic spin embedded in a surface molecular network, Science **317**, 1199 (2007).

[54] S. Loth, M. Etzkorn, C. P. Lutz, D. M. Eigler, and A. J. Heinrich, Measurement of fast electron spin relaxation times with atomic resolution, Science **329**, 1628 (2010).

[55] W. Paul, K. Yang, S. Baumann, N. Romming, T. Choi, C. P. Lutz, and A. J. Heinrich, A scanning tunneling microscope capable of electron spin resonance and pump-probe spectroscopy at mK temperature and in vector magnetic field, Nat. Phys. **13**, 403 (2017).

[56] S. Trishin, C. Lotze, N. Bogdanoff, F. von Oppen, and K. J. Franke, Moiré Tuning of Spin Excitations: Individual Fe Atoms on MoS_2/Au(111), Phys. Rev. Lett. **127**, 236801 (2021).

[57] M. Ternes, Spin excitations and correlations in scanning tunneling spectroscopy, New J. Phys. **17**, 063016 (2015).

[58] S. Trishin, C. Lotze, F. Lohss, G. Franceschi, L. I. Glazman, F. von Oppen, K. J. Franke, Tuning a Two-Impurity Kondo System by a Moiré Superstructure, Phys. Rev. Lett. **130**, 176201 (2023).

[59] Y. Wang, B. Wang, R. Huang, B. Gao, F. Kong, and Q. Zhang, First-principles study of transition-metal atoms adsorption on MoS_2 monolayer, Physica E (Amsterdam) **63**, 276 (2014).

[60] X. Chen, L. Zhong, X. Li, and J. Qi, Valley splitting in the transition-metal dichalcogenide monolayer via atom adsorption, Nanoscale **9**, 2188 (2017).

[61] M. Moro-Lagares, J. Fernández, P. Roura-Bas, M. R. Ibarra, A. A. Aligia, and D. Serrate, Quantifying the leading role of the surface state in the Kondo effect of Co/Ag(111), Phys. Rev. B **97**, 235442 (2018).

[62] R. Žitko and T. Pruschke, Energy resolution and discretization artifacts in the numerical renormalization group, Phys. Rev. B **79**, 085106 (2009).

[63] NRG Ljubljana, https://github.com/rokzitko/nrgljubljana and http://nrgljubljana.ijs.si/.

[64] R. Bulla, T. Costi, and T. Pruschke, The numerical renormalization group method for quantum impurity systems, Rev. Mod. Phys. **80**, 395 (2008).

[65] J. Fernández, P. Roura-Bas, A. Camjayi, and A. A. Aligia, Two-stage three-channel Kondo physics for an FePc molecule on the Au(111) surface, J. Phys.: Condens. Matter **30**, 374003 (2018); A. A. Aligia, Corrigendum: Two-stage three-channel Kondo physics for an FePc molecule on the Au(111) surface, *ibid.* **31**, 029501 (2018).